Original Article

Association between Arterial Stiffness and Cerebral White Matter Lesions in Community-Dwelling Elderly Subjects

Takahiro OHMINE[1,2], Yoshikazu MIWA[1,3], Hiroshi YAO[3,4], Takefumi YUZURIHA[4], Yuki TAKASHIMA[4], Akira UCHINO[5], Fumi TAKAHASHI-YANAGA[1], Sachio MORIMOTO[1], Yoshihiko MAEHARA[2], and Toshiyuki SASAGURI[1]

The presence of cerebral white matter lesions (WMLs) on MRI is suggested to be a predictive factor for vascular dementia and stroke. To investigate the relationship between arterial stiffness and WMLs, we performed brain MRI to evaluate the presence of two subtypes of WML—periventricular hyperintensities (PVH) and deep white matter lesions (DWML)—and furthermore, determined the brachial-ankle pulse wave velocity (ba-PWV) as a marker of arterial stiffness in 132 elderly asymptomatic subjects (49 men and 83 women, 70.3 ± 9.0 years). PVH and DWML were observed in 41 (31.0%) and 53 (40.2%) subjects, respectively. The ba-PWV values were significantly greater in subjects with PVH than in those without. DWML also tended to be associated with ba-PWV, but the correlation was not statistically significant. In multiple logistic regression analysis, age and decreased DBP were independently associated with PVH. ba-PWV was also detected as an independent factor for the appearance of PVH (adjusted odds ratio: 2.84, $p=0.015$) but not DWML. These results indicate that the increase in arterial stiffness contributes to the pathogenesis of PVH rather than DWML. Although further study is needed to clarify the difference between WML subtypes, our study suggests that the measurement of ba-PWV is a simple and useful tool for detecting cerebral arterial dysfunction. (*Hypertens Res* 2008; 31: 75–81)

Key Words: white matter lesion, magnetic resonance imaging, pulse wave velocity, arterial stiffness, periventricular hyperintensity
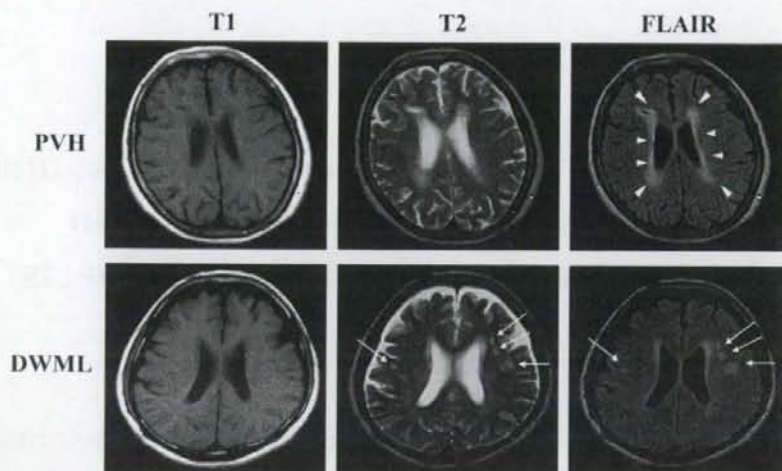
Introduction

Cerebral white matter lesions (WMLs), detected as areas of hyperintensity in T_2-weighted scans and of isointensity in T_1-weighted scans on MRI, are frequently seen in elderly people without apparent neurological symptoms (*1*, *2*). Although the clinical importance of WMLs has not been fully elucidated, the presence of WMLs on MRI was reported to correlate with mental deterioration or cognitive impairment (*3*, *4*), mood disorder (*5*), and gait disturbance (*6*). Previous reports suggested that WMLs are associated with chronic hypoperfusion or ischemia in the white matter (*7*, *8*). It has been shown that WMLs are frequently observed in subjects with traditional cerebrovascular risk factors such as aging, hypertension, or diabetes (*1*, *2*, *9*, *10*) and that the presence of WMLs is an

Fig. 1. *MRI of PVH (upper) and DWML (lower): T_1-weighted (left), T_2-weighted (middle), and FLAIR (right). PVH and DWML were determined as described in the Methods section. Arrowheads and arrows indicate PVH and DWML, respectively.*

independent risk factor for stroke (*11*). WMLs are more frequent in vascular dementia than in other dementias (*12*). Furthermore, several pathological studies reported a thickened intima or atherosclerotic changes of the cerebral arteries in regions containing WMLs (*13, 14*). These observations suggest that the pathogenesis of WMLs is closely associated with arteriosclerosis or atherosclerosis. However, from the perspectives of time and cost, it is not realistic to use MRI for screening early cerebrovascular damage. Recently, pulse wave velocity (PWV) measurements have been found useful for assessing early atherosclerotic change (especially in vascular stiffness) of the vascular wall. An increase in aortic PWV was reported in patients with end-stage renal disease (*15*) and diabetes (*16*), and as a risk factor for cardiovascular and all-cause mortality (*17*). Aortic PWV is also reportedly elevated in patients with stroke (*18*) and a prognostic factor for vascular dementia or cerebral infarction (*19*). Thus, estimations of PWV can be used for both the screening of atherosclerosis and as a predictor of cardiovascular events. Nevertheless, the relationship between PWV and WMLs has not been examined. In the present study, therefore, to test whether or not PWV values are associated with the prevalence of WMLs, we assessed the presence of two distinct types of cerebral WML—periventricular hyperintensities (PVH) and deep white matter lesions (DWML)—in elderly asymptomatic subjects. We also determined the brachial-ankle PWV (ba-PWV), a noninvasive measure of arterial stiffness using an automatic device, and examined its association with the presence of WMLs on MRI.

Methods

Participants

Between August and November in both 2003 and 2004, we examined 144 elderly asymptomatic subjects (52 men and 92 women) living in the rural community of Sefuri village, population 600, in Saga Prefecture, Japan. We randomly contacted inhabitants through the village office by mail, and only those who agreed to participate were enrolled in the study. The positive response rate was 92.3% (144/156). All participants were living independently at home and had a Mini-Mental Status examination score >24. Subjects with an apparent history of stroke, silent brain infarction on MRI, or arrhythmia including atrial fibrillation, or who were suspected of having peripheral arterial disease (ankle-brachial index [ABI, the ratio of ankle pressure to brachial pressure] <0.9) were excluded. Finally, 132 subjects were analyzed. At the time of physical examination, blood pressure (BP), body mass index (BMI), and hematological and biochemical profiles were determined. Smoking status and medical histories were recorded for all participants at the same time. Blood was drawn in the morning after an overnight fast. Fasting blood glucose, HbA1c, triglyceride, total cholesterol, and high-density lipoprotein (HDL)–cholesterol levels were measured using routine laboratory methods. Low-density lipoprotein (LDL)–cholesterol levels were calculated using Friedewald's formula. Hypertension was defined as either systolic BP (SBP) ≥140 mmHg or diastolic BP (DBP) ≥90 mmHg, or current use of an antihypertensive agent. Dyslipidemia was defined as LDL-cholesterol ≥3.6 mmol/L (140 mg/dL) or

Table 1. Characteristics of the Participants

Age, years	70.3±9.0
Male, %	37.1
Habitual smoking, %	28.0
Hypertension, %	54.5
Dyslipidemia, %	15.9
Diabetes, %	6.8
Body mass index, kg/m²	23.4±3.6
SBP, mmHg	136.8±18.7
DBP, mmHg	78.9±9.1
MBP, mmHg	97.4±13.8
PP, mmHg	57.4±16.4
HDL-cholesterol, mmol/L	1.5±0.4
LDL-cholesterol, mmol/L	2.9±0.9
Fasting plasma glucose, mmol/L	5.6±1.4
HbA1c, %	5.2±0.7

Data are shown as frequencies or mean±SD. SBP, systolic blood pressure; DBP, diastolic blood pressure; PP, pulse pressure; HDL, high-density lipoprotein; LDL, low-density lipoprotein.

current use of lipid-lowering agents. Diabetes mellitus was diagnosed as fasting blood glucose ≥7.0 mmol/L (126 mg/dL) or current use of oral anti-diabetic agents. Written informed consent was obtained from all participants. The study protocol was approved by the ethical review committee of the National Hospital Organization Hizen Psychiatric Center.

Assessment of WML

A brain MRI examination was performed with a 1.0 Tesla superconducting magnet (MAGNEX XP, Shimadzu, Tokyo, Japan) using the spin echo technique and fluid attenuated inversion recovery (FLAIR) sequences as described previously (20). Transverse T_1-weighted (T_R/T_E 510/12 ms), T_2-weighted (T_R/T_E 4.300/22 ms), and FLAIR ($T_R/T_I/T_E$ 6,744/1,588/22 ms) images were obtained with a slice thickness of 6 mm separated by a 1 mm interscan gap. WMLs were specified as areas of high signal intensity in T_2-weighted images and isointense areas of normal brain parenchyma in T_1-weighted images obtained at two slices above the level of the pineal body (Fig. 1). A silent lacunar infarction (SBI) was defined as the presence of high signal intensity on a T_2-weighted image and a corresponding obvious low-intensity area on a T_1-weighted image. État criblé was characterized by high signal intensity on the T_2-weighted image and no abnormalities on the T_1-weighted image. The severity of DWML or PVH was classified according to Fazekas et al. (21) as follows. PVH: Grade 0, absent; Grade 1, caps or pencil-thin lining; Grade 2, smooth halo; Grade 3, irregular and extending into the deep white matter. DWML: Grade 0, absent; Grade 1 punctate; Grade 2, beginning confluent; Grade 3, large confluent. For PVH, we determined the presence and severity
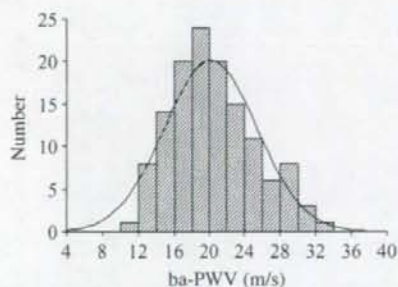
Fig. 2. *The distribution of ba-PWV values. Solid line represents normal distribution.*

using FLAIR images. All scans were reviewed independently by two of the authors (H.Y. and A.U.) blinded to the other clinical data. In the case of disagreement between the raters, a consensus reading was held.

PWV Measurement

Oscillometric ba-PWV was automatically measured using AT form (Nihon-Colin AT, Tokyo, Japan) as described previously (22). This device records a phonocardiogram, an electrocardiogram, a volume pulse form, and arterial blood pressure at bilateral brachia and ankles. The ba-PWV level was calculated by time-phase analysis of the right brachium and ankle. The intra-observer and inter-observer coefficients of variation obtained using 50 subjects were 2.1% and 2.3%, respectively.

Statistical Analysis

Data are presented as means±SD, means±SEM, or frequencies. In a simple regression analysis, Pearson's correlation coefficients were used for continuous variables, and Spearman's correlation coefficients were used for categorical variables. Differences in variables between the groups were assessed with unpaired Student's t-test. Predictive variables, including ba-PWV for the presence of WMLs, were analyzed using a logistic regression analysis. The independent variables were age, sex (men: 1, women: 0), body mass index, habitual smoking (yes: 1, no: 0), antihypertensive therapy (yes: 1, no: 0), DBP, pulse pressure (PP), HDL-cholesterol, LDL-cholesterol, HbA1c, and ba-PWV. $p < 0.05$ was considered statistically significant. All statistical analyses were performed with StatView Version 5.0 (SAS Institute, Cary, USA).

Results

The participants' characteristics are summarized in Table 1. Their ages ranged from 55 to 89 years. About 76% of hyper-
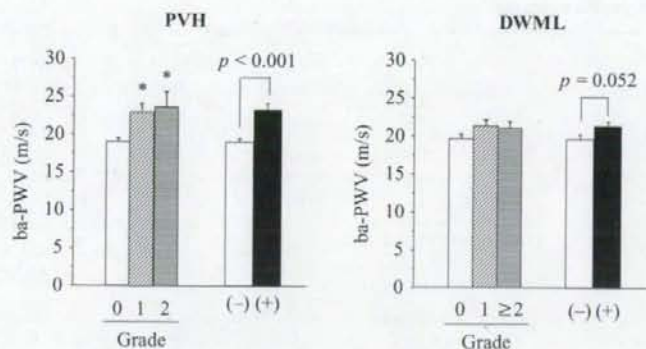
Fig. 3. *The values of ba-PWV in subjects classified by the severity of DWML or PVH according to Fazekas et al. (21). Statistical significance among groups was assessed with ANOVA. Statistical significance between subjects with (+) or without (−) WMLs was assessed with unpaired Student's t-test. Error bars indicate SEM. *p < 0.01 vs. Grade 0.*
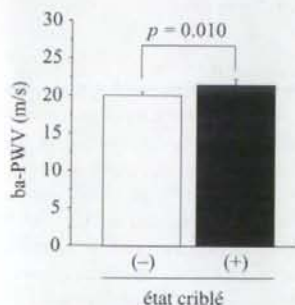
Fig. 4. *The age-adjusted values of ba-PWV in subjects with (+) or without (−) état criblé. Error bars indicate SEM.*

tensive subjects (55 of 72 subjects) were being treated with an antihypertensive agent. PVH and DWML were observed in 41 subjects (Grade 1, 35 subjects; Grade 2, 6 subjects) and 53 subjects (Grade 1, 36 subjects; Grade 2, 16 subjects; Grade 3, 1 subject), respectively. No subjects had Grade 3 PVH.

In a simple correlation analysis, the presence of PVH was positively correlated with age ($r=0.44$, $p<0.001$), and inversely correlated with DBP ($r=-0.27$, $p=0.002$), and MBP ($r=-0.19$, $p=0.026$). DWML was also associated with age ($r=0.28$, $p=0.001$), and DBP ($r=-0.18$, $p=0.044$). Other traditional atherosclerotic risk factors, such as sex, body mass index, SBP, PP, fasting plasma glucose level, and HbA1c showed no significant correlations with WMLs. Age- and sex-adjusted regression analysis also showed no significant correlation between traditional atherosclerotic risk factors and WMLs (data not shown).

The mean ba-PWV was 20.2±5.2 (m/s). The ba-PWV values were normally distributed (Fig. 2) and did not differ significantly between genders (men: 20.0±5.3 m/s, women:

20.3±5.2 m/s). When subjects were divided into two groups according to the presence of WMLs, ba-PWV was significantly greater in subjects with PVH than in those without (Fig. 3). DWML also tended to be associated with ba-PWV, but this correlation was not statistically significant. We also assessed the presence of *état criblé* (dilatation of perivascular space) as a surrogate marker of stiffening of small arteries and investigated its association with ba-PWV. Subjects with *état criblé* tended to have greater age-adjusted ba-PWV values than those without, but the difference was not significant (Fig. 4). In a multiple logistic regression analysis including age, sex, and other traditional atherosclerotic risk factors (BMI, smoking, antihypertensive agent, DBP, PP, LDL-cholesterol, HDL-cholesterol, and HbA1c), ba-PWV was detected as an independent factor for the appearance of PVH (odds ratio 2.84, $p=0.015$) (Table 2). Aging and decreased DBP were also independently associated with PVH. The association between ba-PWV and PVH did not change when SBP and MBP were forced into the model instead of DBP.

Discussion

In the present study, we showed that ba-PWV is associated with the appearance of WMLs on MRI in elderly asymptomatic subjects. In particular, the increase in ba-PWV is an independent predictor for the prevalence of PVH.

PWV, often used as a marker of arterial stiffness, is useful for detecting early atherosclerotic changes in the vascular wall. Increased aortic PWV was reported as a risk factor for cardiovascular and all-cause mortality (17), vascular dementia, and stroke (18) independent of other traditional atherosclerotic risk factors. ba-PWV, a noninvasively measurable PWV, was strongly associated with aortic PWV (23) and was elevated in subjects with diabetic complications including cerebral infarction (24), abdominal aortic calcification (22), and coronary artery disease (25). Although the pathogenesis

Table 2. Multiple Logistic Regression Analyses Relating to the WMLs

	PVH		DWML	
	OR (95% CI)	p	OR (95% CI)	p
Age	2.58 (1.36–4.89)	0.004	1.68 (0.98–2.86)	0.060
Sex	1.12 (0.58–2.16)	0.723	1.34 (0.78–2.29)	0.277
Habitual smoking	1.32 (0.67–2.57)	0.421	1.04 (0.61–1.76)	0.889
Body mass index	1.14 (0.63–1.98)	0.628	1.35 (0.86–2.12)	0.194
Diastolic blood pressure	0.48 (0.26–0.84)	0.010	0.68 (0.44–1.04)	0.080
Pulse pressure	0.90 (0.54–1.51)	0.706	0.92 (0.58–1.45)	0.729
LDL-cholesterol	0.91 (0.50–1.62)	0.729	1.35 (0.85–2.12)	0.212
HDL-cholesterol	1.03 (0.60–1.77)	0.930	0.94 (0.60–1.47)	0.815
HbA1c	1.25 (0.76–2.07)	0.377	1.01 (0.65–1.57)	0.959
Antihypertensive therapy	0.66 (0.38–1.14)	0.141	1.17 (0.75–1.82)	0.495
ba-PWV	2.84 (1.02–7.89)	0.015	1.21 (0.47–3.16)	0.488

WMLs, white matter lesions; PVH, periventricular hyperintensities; DWML, deep white matter lesions; OR, odds ratio; CI, confidence interval; LDL, low-density lipoprotein; HDL, high-density lipoprotein. Adjusted ORs for continuous variables were indicated for 1 SD.

of WMLs remains largely unknown, it is generally believed to involve chronic hypoperfusion or ischemia in cerebral circulation (7). A recent report indicated that the severity of WMLs is an independent predictor of symptomatic stroke due to arteriolosclerosis, and that the progression of WMLs is associated with subsequent stroke in patients with initially mild WMLs (26).

Supposing that the presence of WMLs reflects early atherosclerotic changes in the cerebral arteries, our result showing an association between ba-PWV and PVH is reasonable. However, the ba-PWV association differed between PVH and DWML. Although we cannot well explain this difference, it may be that PWV is transported *via* the CSF in subependymal regions and therefore affects PVH even more. Pathohistological features may also be distinct between these two types of WMLs. Fazekas *et al.* (13) reported intimal thickening of the arterial wall in the region of DWML. With regard to PVH, severe, but not mild or moderate, PVH showed arteriosclerotic changes in the cerebral arteries. Since this series did not include subjects with a high grade of PVH according to their MRI classification (21), our subjects may not have had severe arteriosclerosis in the cerebral arteries. However, the important issue is that Fazekas *et al.* (21) assessed morphological change (*i.e.*, vascular wall thickening) as a marker of arteriosclerosis. Atherosclerosis consists of morphological change (atherosis) and functional change (sclerosis) of the vessel wall. PWV may finally reflect both changes, because it is associated with the consequence of advanced arteriosclerosis, such as end-stage renal disease (15), cardiovascular mortality (17), and stroke (18) although, in the early phase of atherosclerosis, it mainly reflects functional rather than morphological change in the vascular wall. The correlation between ba-PWV and mild to moderate PVH in the present study may show the functional disturbance of the cerebral arteries. Indeed, a white matter edema that induces demyelination and reactive gliosis is frequently seen in the region of PVH. The

increase in ba-PWV may be associated with a functional disturbance, such as an increase in endothelial permeability in irrigated vessels of PVH. In addition, a previous study showed that aortic calcification in middle age predicted PVH but not DWML in the elderly (27). Since aortic calcification is closely correlated with aortic PWV (20) and pulse pressure (28), the increased stiffness in the conduit large artery may contribute to the pathogenesis of PVH.

To our knowledge, only one group has reported a relationship between aortic PWV and PVH grades rated according to Shimada *et al.* (29), although there was no significant correlation between them (30). However, this WML grading scale did not distinguish between PVH and DWML. Furthermore, the subjects analyzed were over 80 years old and had severe PVH (average grade =2.2±0.9 in normotensive subjects). Therefore, the possibility that DWMLs were involved in severe PVH cannot be excluded. These factors might have led to their negative results. Conversely, we accurately distinguished between PVH and DWML because our population had modest WMLs and we used the Fazekas classification. Consequently, we found a significant association between ba-PWV and PVH.

One limitation in the present study would be the frequent use of antihypertensive agents among hypertensive subjects. Hypertension is one of the most important risk factors for WMLs; moreover, a recent study reported that optimal blood pressure control suppressed the progression of both PVH and DWML (9). Especially in the elderly, peripheral amplification of the arterial wall is gradually reduced with structural arterial stiffening. These changes lead to higher SBP, lower DBP, and wider PP, *i.e.*, isolated systolic hypertension. Indeed, several groups reported that SBP and PP were positively correlated, and DBP inversely correlated, with cardiovascular risk in the elderly (31, 32). We did not find any apparent contribution of SBP or PP to WMLs in our population, whereas decreased DBP was an independent risk factor

for PVH and also tended to be associated with DWML (Table 2). About 80% of hypertensive subjects were treated with antihypertensive agents and were relatively well controlled in the present study. Therefore, the effects of SBP and PP may be diminished. On the other hand, DBP may remain as an independent risk factor, since antihypertensive therapy is less effective for DBP than SBP.

In conclusion, we reported for the first time that increased ba-PWV is closely associated with the appearance of PVH in an elderly asymptomatic population. Although it is difficult to use MRI for health screening, our results suggest that ba-PWV measurement is a simple and useful tool for predicting early cerebrovascular dysfunction.

Acknowledgements

References

1. de Leeuw FE, de Groot JC, Athten E, *et al*: Prevalence of cerebral white matter lesions in elderly people: a population based magnetic resonance imaging study. The Rotterdam Scan Study. *J Neurol Neurosurg Psychiatry* 2001; **70**: 9–14.
2. Ylikoski A, Erkinjuntti T, Raininko R, Sarna S, Sulkava R, Tilvis R: White matter hyperintensities on MRI in the neurologically nondiseased elderly. Analysis of cohorts of consecutive subjects aged 55 to 85 years living at home. *Stroke* 1995; **26**: 1171–1177.
3. Fukuda H, Kobayashi S, Okada K, Tsunematsu T: Frontal white matter lesions and dementia in lacunar infarction. *Stroke* 1990; **21**: 1143–1149.
4. Breteler MM, van Amerongen NM, van Swieten JC, *et al*: Cognitive correlates of ventricular enlargement and cerebral white matter lesions on magnetic resonance imaging. The Rotterdam Study. *Stroke* 1994; **25**: 1109–1115.
5. Greenwald BS, Kramer-Ginsberg E, Krishnan KR, Ashtari M, Auerbach C, Patel M: Neuroanatomic localization of magnetic resonance imaging signal hyperintensities in geriatric depression. *Stroke* 1998; **29**: 613–617.
6. Baloh RW, Yue Q, Socotch TM, Jacobson KM: White matter lesions and disequilibrium in older people. I. Case-control comparison. *Arch Neurol* 1995; **52**: 970–974.
7. Braffman BH, Zimmerman RA, Trojanowski JQ, Gonatas NK, Hickey WF, Schlaepfer WW: Brain MR: pathologic correlation with gross and histopathology. 2. Hyperintense white-matter foci in the elderly. *AJR Am J Roentgenol* 1988; **151**: 559–566.
8. Schmidt R, Fazekas F, Kapeller P, Schmidt H, Hartung HP: MRI white matter hyperintensities: three-year follow-up of the Austrian Stroke Prevention Study. *Neurology* 1999; **53**: 132–139.
9. de Leeuw FE, de Groot JC, Oudkerk M, *et al*: Hypertension and cerebral white matter lesions in a prospective cohort study. *Brain* 2002; **125**: 767–772.
10. Vermeer SE, Hollander M, van Dijk EJ, Hofman A, Koudstaal PJ, Breteler MM: Silent brain infarcts and white matter lesions increase stroke risk in the general population: the Rotterdam Scan Study. *Stroke* 2003; **34**: 1126–1129.
11. Barber R, Scheltens P, Gholkar A, *et al*: White matter lesions on magnetic resonance imaging in dementia with Lewy bodies, Alzheimer's disease, vascular dementia, and normal aging. *J Neurol Neurosurg Psychiatry* 1999; **67**: 66–72.
12. Yao H, Sadoshima S, Kuwabara Y, Ichiya Y, Fujishima M: Cerebral blood flow and oxygen metabolism in patients with vascular dementia of the Binswanger type. *Stroke* 1990; **21**: 1694–1699.
13. Fazekas F, Kleinert R, Offenbacher H, *et al*: Pathologic correlates of incidental MRI white matter signal hyperintensities. *Neurology* 1993; **43**: 1683–1689.
14. Leifer D, Buonanno FS, Richardson EP Jr: Clinicopathologic correlations of cranial magnetic resonance imaging of periventricular white matter. *Neurology* 1990; **40**: 911–918.
15. Mourad JJ, Pannier B, Blacher J, *et al*: Creatinin clearance, pulse wave velocity, carotid compliance and essential hypertension. *Kidney Int* 2001; **59**: 1834–1841.
16. Suzuki E, Kashiwagi A, Nishio Y, *et al*: Increased arterial wall stiffness limits in the lower extrimities in type 2 diabetic patient. *Diabetes Care* 2001; **24**: 2107–2114.
17. Laurent S, Boutouyrie P, Asmar R, *et al*: Aortic stiffness is an independent predictor of all-cause and cardiovascular mortality in hypertensive, patients. *Hypertension* 2001; **37**: 1236–1241.
18. Lehmann ED, Hopkins KD, Jones RL, Rudd AG, Gosling RG: Aortic distensibility in patients with cerebrovascular disease. *Clin Sci (Lond)* 1995; **89**: 247–253.
19. Laurent S, Katsahian S, Fassot C, *et al*: Aortic stiffness is an independent predictor of fatal stroke in essential hypertension. *Stroke* 2003; **34**: 1203–1206.
20. Takashima Y, Yao H, Koga H, *et al*: Frontal lobe dysfunction caused by multiple lacunar infarction in community-dwelling elderly subjects. *J Neurol Sci* 2003; **214**: 37–41.
21. Fazekas F, Chawluk JB, Alavi A, Hurtig HI, Zimmerman RA: MR signal abnormalities at 1.5 T in Alzheimer's dementia and normal aging. *AJR Am J Roentgenol* 1987; **149**: 351–356.
22. Nakamura U, Iwase M, Nohara S, Kanai H, Ichikawa K, Iida M: Usefulness of brachial-ankle pulse wave velocity measurement: correlation with abdominal aortic calcification. *Hypertens Res* 2003; **26**: 163–167.
23. Yamashina A, Tomiyama H, Takeda K, *et al*: Validity, reproducibility, and clinical significance of noninvasive brachial-ankle pulse wave velocity measurement. *Hypertens Res* 2002; **25**: 359–364.
24. Ogawa O, Onuma T, Kubo S, Mitsuhashi N, Muramatsu C, Kawamori R: Brachial-ankle pulse wave velocity and symptomatic cerebral infarction in patients with type 2 diabetes: a cross-sectional study. *Cardiovasc Diabetol* 2003; **2**: 10.
25. Yufu K, Takahashi N, Anan F, Hara M, Yoshimatsu H, Saikawa T: Brachial arterial stiffness predicts coronary atherosclerosis in patients at risk for cardiovascular diseases. *Jpn Heart J* 2004; **45**: 231–242.
26. Yamauchi H, Fukuda H, Oyanagi C: Significance of white matter high intensity lesions as a predictor of stroke from arteriolosclerosis. *J Neurol Neurosurg Psychiatry* 2002; **72**:

576–582.

27. de Leeuw FE, de Groot JC, Oudkerk M, *et al*: Aortic atherosclerosis at middle age predicts cerebral white matter lesions in the elderly. *Stroke* 2000; **31**: 425–429.

28. Miwa Y, Tsushima M, Arima H, Kawano Y, Sasaguri T: Pulse pressure is an independent predictor for the progression of aortic wall calcification in patients with controlled hyperlipidemia. *Hypertension* 2004; **43**: 536–540.

29. Shimada K, Kawamoto A, Matsubayashi K, Ozawa T: Silent cerebrovascular disease in the elderly. Correlation with ambulatory pressure. *Hypertension* 1990; **16**: 692–699.

30. O'Sullivan C, Duggan J, Lyons S, Thornton J, Lee M, O'Brien E: Hypertensive target-organ damage in the very elderly. *Hypertension* 2003; **42**: 130–135.

31. Franklin SS, Larson MG, Khan SA, *et al*: Does the relation of blood pressure to coronary heart disease risk change with aging? The Framingham Heart Study. *Circulation* 2001; **103**: 1245–1249.

32. Wang J-G, Staessen JA, Gong L, Liu L, Systolic Hypertension in China (Syst-China) Collaborative Group: Chinese trial on isolated systolic hypertension in the elderly. *Arch Intern Med* 2000; **160**: 211–220.

Knockout of the *l-pgds* gene aggravates obesity and atherosclerosis in mice

Reiko Tanaka [a,b], Yoshikazu Miwa [a,*], Kin Mou [a], Morimasa Tomikawa [c], Naomi Eguchi [d], Yoshihiro Urade [d], Fumi Takahashi-Yanaga [a], Sachio Morimoto [a], Norio Wake [b], Toshiyuki Sasaguri [a]

[a] Department of Clinical Pharmacology, Faculty of Medical Sciences, Kyushu University, 3-1-1, Maidashi, Higashi-ku, Fukuoka 812-8582, Japan
[b] Department of Obstetrics and Gynecology, Faculty of Medical Sciences, Kyushu University, Fukuoka, Japan
[c] Department of Future Medicine and Innovative Medical Information, Faculty of Medical Sciences, Kyushu University, Fukuoka, Japan
[d] Department of Molecular Behavioral Biology, Osaka Bioscience Institute, Suita, Japan

ARTICLE INFO

ABSTRACT

This study was designed to determine whether lipocalin type-prostaglandin D synthase (*l-pgds*) deficiency contributes to atherogenesis using gene knockout (KO) mice. A high-fat diet was given to 8-week-old C57BL/6 (wild type; WT), *l-pgds* KO (LKO), *apolipoprotein E (apo E)* KO (AKO) and *l-pgds/apo E* double KO (DKO) mice. The *l-pgds* deficient mice showed significantly increased body weight, which was accompanied by increased size of subcutaneous and visceral fat tissues. Fat deposition in the aortic wall induced by the high-fat diet was significantly increased in LKO mice compared with WT mice, although there was no significant difference between AKO and DKO mice. In LKO mice, atherosclerotic plaque in the aortic root was also increased and, furthermore, macrophage cellularity and the expression of pro-inflammatory cytokines such as interleukin-1β and monocyte chemoattractant protein-1 were significant increased. In conclusion, *l-pgds* deficiency induces obesity and facilitates atherosclerosis, probably through the regulation of inflammatory responses.

© 2008 Elsevier Inc. All rights reserved.

Lipocalin-type prostaglandin D synthase (L-PGDS) is the enzyme that converts PGH_2 into PGD_2 in the process of an arachidonic acid metabolism. The synthesized PGD_2 is further non-enzymatically metabolized to the PGJ_2 series including PGJ_2, Δ^{12}-PGJ_2 and 15-deoxy-$\Delta^{12,14}$-PGJ_2 ($15d$-PGJ_2) [1]. Because L-PGDS is highly expressed in the central nervous system, its role in neurological disorders has been well studied [2–4]. In addition, recent studies have revealed that L-PGDS is constitutively expressed in the vascular endothelium [5] and that the downstream PGs, PGD_2 and the PGJ_2 series mainly act as protective factors for blood vessels [6]. The role of $15d$-PGJ_2 has received particular attention because it was reported as a natural ligand of the nuclear receptor peroxisome proliferator-activated receptor-γ (PPARγ) that induces the differentiation of adipose cells and macrophages [7,8], which contribute to insulin resistance. $15d$-PGJ_2 has been shown to be a unique material that is able to protect the vessel wall from injurious stimuli by controlling cell fate such as proliferation, differentiation and apoptosis, and by inhibiting inflammation in the vascular wall [6,9,10].

L-PGDS is secreted into the blood and urine, and several clinical studies have suggested a close association between L-PGDS levels and cardiovascular disease or its risk factors. The urinary L-PGDS level is significantly increased in patients with hypertension [11].

The L-PGDS concentration is increased in both serum and urine in diabetic patients and blood sugar control reversed the increase in urinary excretion of L-PGDS [12]. We previously reported that the serum L-PGDS level increases with aging and is associated with subclinical atherosclerosis as evaluated by the maximal intima-media complex thickness of the common carotid artery (C-IMT *max*) and by the pulse wave velocity [13]. In addition, we have identified single nucleotide polymorphisms (SNPs) in the *l-pgds* gene in Japanese people, and showed that a common SNP 4111A>C influences C-IMT *max* [14]. These observations strongly suggest the importance of L-PGDS in the pathogenesis of atherosclerosis; however, its role in vivo has not been well investigated.

Therefore, in the present study, to clarify the pathophysiologic role of L-PGDS in atherosclerosis, we investigated the effects of a high-fat diet on atherosclerosis and related parameters in *l-pgds* gene knockout (LKO) mice. We also crossed these mice with *apolipoprotein E (apo E)* knockout (AKO) mice, which are frequently used as a model of atherosclerosis, to generate a double knockout (DKO), and similarly investigated this phenotype.

Methods

Animals. All animal experiments were approved by the Committee on the Ethics of Animal Experiments, Kyushu University Graduate School of Medical Sciences. LKO mice were generated as previously described [4]. AKO mice and C57BL/6 (wild type, WT)

* Corresponding author. Fax: +81 92 642 6084.
  E-mail address: ymiwa@clipharm.med.kyushu-u.ac.jp (Y. Miwa).

mice were obtained from Jackson Laboratory (Bar Harbor, ME). DKO mice were generated by mating LKO mice with AKO mice. After genotyping by polymerase chain reaction analysis, littermates from the F2 generation of this crossbreed were used to establish DKO mating, and the resulting progeny was used in our study. All animals were of pure (9-generation backcross) C57BL/6 genetic background. Male mice were fed a normal chow diet until 8 weeks of age, after which they received a high-fat diet containing 30% fat (Oriental Yeast Co., Tokyo, Japan) for 20 weeks. Mice were maintained in an air-conditioned room (25 °C; humidity 50%) with a 12 h light and dark cycle. Animals had free access to diet and drinking water but were not fed overnight prior to the experiments.

During the high-fat feeding, body weight and systolic blood pressure (BP) were measured every 4 weeks. Systolic BP was examined by tail-cuff plethysmography (BP98-A, Softron Co., Tokyo, Japan) on conscious restrained mice. Each measurement was performed five times, and values were averaged and recorded. Food intake was monitored daily for a period of 7 days in single-housed mice. After a week of acclimatization to the new environment, the amount of diet ingested was calculated as the difference between the weight of the food remaining in the food bin and the amount of pre-weighed food added the day before. Serum levels of cholesterols, triglyceride, creatinine and adiponectin were determined using blood samples collected from mice at 12 weeks after starting the high-fat diet.

Intraperitoneal glucose tolerance tests were performed in mice fasted for 16 h. Blood was collected before and after intraperitoneal injection of glucose (1 g/kg) at 15, 30, 60, 90 and 120 min. Intraperitoneal insulin tolerance test was performed after mice were fasted for 5 h. Blood glucose levels were measured prior to the injection of insulin (1.0 U/kg; Novolin®, Novo Nordisk Pharmaceuticals, Inc., Princeton, NJ) and at 15, 30, 60, 90 and 120 min after injection.

Magnetic resonance imaging (MRI) studies. In vivo MRI scanning was performed using a 0.3-T open MRI (AIRIS II, Hitachi Medico., Tokyo, Japan) to determine body fat distribution. Mice were anesthetized with pentobarbital (50 μg/g) and placed in a coil. T1-weighted SE sequence (TR/TE = 450/14 ms; FOV 85 mm; matrix 512 × 512; slice thickness 2 mm) was used to acquire 14 transverse slices. To evaluate the volumes of visceral and subcutaneous adipose tissue compartments, digital images were captured and hyper-intense fat was manually segmented and areas calculated as pixels using NIH Image J software (version 1.6.0, National Institute of Health, ML). The average values obtained from six consecutive slices between the middle of the right kidney to urinary bladder were defined as the fat tissue volume.

Measurements of adipocyte sizes. To determine adipocyte sizes of visceral and subcutaneous fat, the cross-sectional area of adipocytes was measured on paraffin-embedded hematoxylin–eosin-stained sections as previously described [15]. After converting the image of adipose tissue under the microscope to a binary image, each adipocyte from five randomly chosen fields (approximately 100 cells per mouse) was manually segmented and the areas calculated as pixels using NIH Image J software.

En face evaluation of atherosclerotic lesions. After the mice were fed with a high-fat diet for 20 weeks, they were anesthetized with pentobarbital and perfused with Krebs-Ringer solution, and the aorta was dissected from the aortic valve to the iliac bifurcation under a light microscope. The whole aorta was fixed in 10% formaldehyde for over 24 h, and opened longitudinally and pinned onto a black wax surface. To identify lipid-rich intraluminal lesions, the aorta was stained for 30 min in a saturated Oil-Red-O solution at room temperature. Digital images of the aortic lumen en face under the microscope were captured and saved on a computer and the index of atherosclerotic formation ([total lesion area/total sur-

face area] × 100%) in the aortic arch was calculated for each aorta using NIH Image J software.

Histological examination of the aortic root. The aortic root was dissected and placed in 10% formaldehyde for 24 h and then transferred to 10–30% sucrose solution for 3 days. After embedding in OCT compound (Tissue-Tek), 10-μm-thick sections of the aortic roots were cut using a cryostat at −20 °C. Some of the sections were stained for 15 min in a saturated Oil-Red-O solution at room temperature and counterstained with hematoxylin. For quantitative estimation of the plaque contents, we analyzed the Oil-Red-O-stained areas as previously described [16] using NIH Image J software. The remaining sections were used for immunohistochemical analysis using the following antibodies: monoclonal anti-CD68 (AbD Serotec, Kidlington, UK), polyclonal anti-macrophage chemoattractant protein-1 (MCP-1) (sc-1785, Santa-Cruz, CA) and polyclonal anti-IL-1β (sc-7884; Santa-Cruz). After blocking endogenous peroxidase with 3% H_2O_2 in methanol for 30 min, serial 5-μm-thick cryosections of the aortic root were incubated with each antibody (1:100) overnight at 4 °C. The sections were treated with secondary biotinylated antibodies and incubated with streptavidin labeled with horseradish peroxidase using a Histofine SAB-PO Kit (Nichirei Co., Tokyo, Japan). The sections were then counterstained with hematoxylin. Under the microscope, percentages of stained cells from five randomly chosen fields were manually calculated.

Statistical analysis. Differences between groups were determined by two-tailed Student's *t*-test or one-way analysis of variance (ANOVA). When a significant difference was observed in ANOVA, the difference between two groups was analyzed by post hoc analysis. $P < 0.05$ was considered to be significant.

Results

Effect of l-pgds deficiency on phenotype

After the mice were fed a high-fat diet for 12 weeks from 8-weeks-old, the body weight of *l-pgds*-deficient (LKO and DKO) mice was significantly increased compared with the respective control (WT and AKO) mice (Table 1). When we compared diet consumption among the mice, food intake was significantly lower in *apo* E-deficient (AKO and DKO) mice compared with the WT and LKO mice, whereas *l-pgds* deficiency did not affect food intake. The body weight of *apo* E-deficient mice was also relatively lower but not statistically significant. Although the levels of systolic BP were not influenced by genotype, the serum levels of total cholesterol, LDL-cholesterol and triglyceride were significantly higher in *apo* E-deficient (AKO and DKO) mice. The *l-pgds* deficiency tended to increase total and LDL-cholesterol and triglyceride, although this was not statistically significant. HDL-cholesterol was relatively lower in DKO mice compared with AKO mice, but no difference was observed between WT and LKO mice. Because a recent report [17] showed that *l-pgds* KO mice become glucose intolerant and insulin resistant, we performed an intraperitoneal glucose tolerance test and insulin tolerance test. However, *l-pgds* deficiency did not significantly affect glucose or insulin tolerance (data not shown). Similarly, *l-pgds* deficiency did not affect the serum level of adiponectin, which is an insulin-sensitizing hormone that is exclusively expressed in adipose tissues (Table 1).

Next, to compare the fat tissue volume between *l-pgds*-deficient mice and control mice, we performed abdominal MRI using an open MRI scanner. As shown in Fig. 1A, we evaluated the volumes of visceral and subcutaneous adipose tissue compartments from six consecutive slices between the center of the right kidney (left) and the urinary bladder (right). Significant increases in volume of subcutaneous and visceral fat tissues were observed in MRI images in *l-pgds*-deficient (LKO and DKO) mice (Fig. 1B). These results

Table 1
Characteristics of mice (at 20-week-old).

	WT	LKO	AKO	DKO
Number	8	8	6	6
Food intake (g/week)	31 (1.0)	30 (1.0)	26 (1.5)*	22 (0.7)*
Weight (g)	37.1 (1.4)	46.7 (1.9)*	34.5 (1.2)	40.7 (1.0)†
Systolic blood pressure (mm Hg)	104.6 (5.1)	103.6 (7.3)	101.6 (5.0)	111.4 (7.0)
Total cholesterol (mg/dL)	153.2 (17.2)	189.2 (50.6) *	427.5 (77.7)*	485.7(25.1)*
LDL-cholesterol (mg/dL)	18.0 (3.0)	24.5 (7.5)	124.0 (23.1)*	139.0 (3.6)*
HDL-cholesterol (mg/dL)	61.6 (10.0)	63.3 (8.1)	45.5 (10.1)	38.0 (3.8)
Triglyceride (mg/dL)	12.3 (1.6)	12.7 (2.2)	48.3 (17.0)*	68.0 (12.4)*
Adiponectin (mg/mL)	9.6 (2.4)	10.1 (2.6)	17.3 (1.8)*	18.4 (3.3)

WT, wild type mice; LKO, l-pgds knockout mice; AKO, apo E knockout mice; DKO, l-pgds/apo E double knockout mice; LDL, low density lipoprotein; HDL, high density lipoprotein.
Data represent means (SE).
* P < 0.05 vs WT.
† P < 0.05 vs AKO.
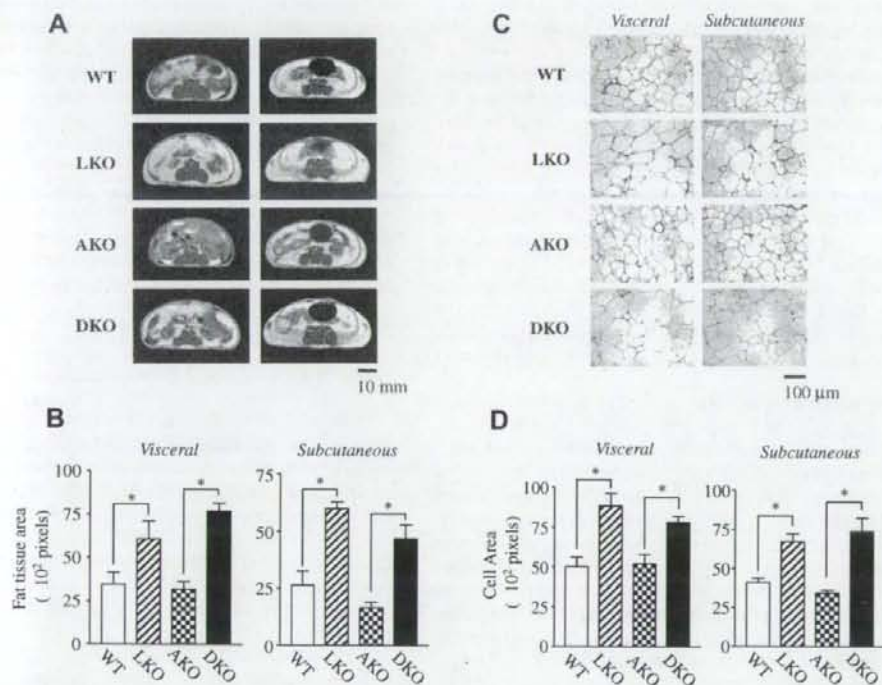
Fig. 1. (A) Abdominal open MRI transverse section of 20-week-old mice (maintained on a high-fat diet for 12 weeks). Left panel: center of the right kidney level; right panel: urinary bladder level. (B) Quantitative analyses of visceral and subcutaneous fat compartments. Areas of fat tissue were calculated as described in Methods. Data represent means ± SE (n = 6–8; *P < 0.01). (C) Representative hematoxylin–eosin-stained sections of visceral and subcutaneous fat in WT and LKO mice. Adipocyte sizes were calculated as described in Methods. Data represent means ± SE (n = 6; *P < 0.01).

were similar to the analysis of fat tissue weight obtained from sacrificed mice (data not shown).

We also compared the adipocyte sizes among mice. Adipocytes in visceral and subcutaneous fat isolated from l-pgds-deficient mice were significantly larger in size than those from WT and AKO mice (Fig. 1C and D).

Effect of l-pgds deficiency on atherosclerosis

Next, we evaluated the effect of l-pgds deficiency on atherosclerosis by investigating lipid depositions in the aortic wall and in cross-sections of the aortic root. As shown in Fig. 2A, Oil-Red-O staining in the longitudinally opened aortas showed a significant

increase in atherosclerotic lesion area in LKO mice compared with WT mice after 20 weeks of high-fat diet feeding. Although greater increases in lipid deposition were observed in AKO and DKO mice, this was not statistically significant. Similarly, Oil-Red-O-stained atherosclerotic plaque area in the aortic root was increased in LKO mice compared with WT mice (Fig. 2B), but there was no difference between AKO and DKO mice (data not shown).

Effects of l-pgds deficiency on inflammatory response

The modulation of vascular remodeling mediated by inflammation is a key event in the progression of atherosclerosis. It has been reported that L-PGDS and its enzymatic products
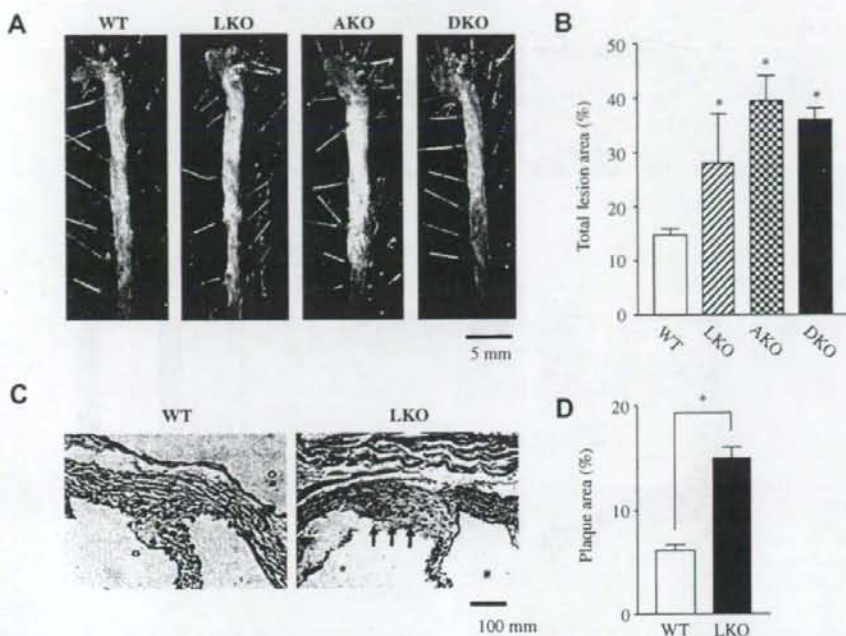
Fig. 2. Atherosclerotic lesions in 28-week-old mice (maintained on a high-fat diet for 20 weeks). (A) Lipid depositions in the aortic wall. Representative photomicrographs of longitudinally opened aortas between the subclavian and iliac branches stained with Oil-Red-O. (B) Quantitative analyses of lipid deposition in the aortic arch calculated as the percentage of the lesion area of the total vascular wall. Data represent means ± SE ($n = 6$; $^*P < 0.05$ vs WT). (C) Atherosclerotic lesions in the aortic root. Representative cross-sections of the aortic root stained with Oil-Red-O and hematoxylin in WT and LKO mice (arrows: lipid staining in red). (D) Quantitative analyses of atherosclerotic lesions calculated as the percentage of the Oil-Red-O stained area of the total aortic root. Data represent means ± SE for lesion area in five sections for each animal ($n = 6$; $^*P < 0.01$).

PGD_2/PGJ_2 have anti-inflammatory actions [7]. Therefore, to examine the effect of *l-pgds* deficiency on inflammation, we compared the infiltration of macrophages in the atherosclerotic lesions in aortic root sections between WT and LKO mice. The number of macrophages stained with anti-CD68 antibody was increased in LKO mice compared with WT mice (Fig. 3A). Furthermore, as shown in Fig. 3B, the expression of pro-inflammatory cytokines such as monocyte chemoattractant protein-1 (MCP-1) and interleukin-1β (IL-1β) in aortic root sections were also markedly enhanced in LKO mice.

Discussion

Here, we showed that *l-pgds* deficiency increases body weight, which is accompanied with an increase in fat tissue volume in a high-fat environment. *l-pgds* deficiency also facilitates atherosclerosis, although this effect occurred to a lesser than in *apo E* deficiency.

The association between L-PGDS and obesity has not been well studied. However, several previous studies suggest that downstream PGs of L-PGDS, i.e., PGD_2 and PGJ_2 contribute to adipocyte differentiation or lipid metabolism, both of which are important in the pathogenesis of obesity through activation of PPARs. In particular, 15d-PGJ_2 stimulates the differentiation of adipose cells through PPARγ, which is abundantly expressed in adipocytes and functions as a key regulator of adipocyte differentiation. Considering these observations, the lack of *l-pgds* may inhibit downstream PG generation in adipose tissue, resulting in the enlargement of adipocytes and concomitant increase in fat tissue volume. Further studies are required to clarify the role of L-PGDS in the pathogenesis of obesity.

On the other hand, PPARγ plays a major role in insulin sensitivity. PPARγ increases small adipocytes by stimulating adipocyte differentiation and enhances expression of the insulin-sensitizing hormone adiponectin. A previous study [17] reported that LKO mice fed a diabetogenic diet were insulin resistant, glucose intolerant and had low serum adiponectin levels. In our study, the high-fat diet increased body weight and induced fat cell enlargement in LKO mice; however, it did not have a significant effect on insulin sensitivity or serum adiponectin levels. Although we are not able to fully explain this discrepancy, differences in diet compositions might be responsible for the inconsistent results. Very recently, the same group reported that L-PGDS stimulates glucose transport via enhanced translocation of the insulin-responsive glucose transporter GLUT4 [18]. However, since there are no other reports to have examined the effect of L-PGDS on glucose metabolisms, further studies are required to clarify this issue.

Because L-PGDS belongs to the lipocalin superfamily, a group of proteins that bind and transport small lipophilic molecules, L-PGDS may play a role in lipid transport. Indeed, we found an association between L-PGDS and serum lipid levels in the clinical studies. Serum L-PGDS levels were inversely associated with HDL-cholesterol [13] and a gene polymorphism of human *l-pgds* gene (4111 A>C) was associated with HDL-cholesterol levels [14]. In the present study, LKO mice showed relatively lower HDL-cholesterol and higher LDL-cholesterol levels, although these findings were not statistically significant. Based on these observations, even if L-PGDS contributes to lipid metabolism, its role does not seem to be important.

Our data also provide evidence for the atheroprotective functions of L-PGDS. Although the data were preliminary, Ragolia et al. [17] reported that LKO mice fed a diabetogenic diet showed
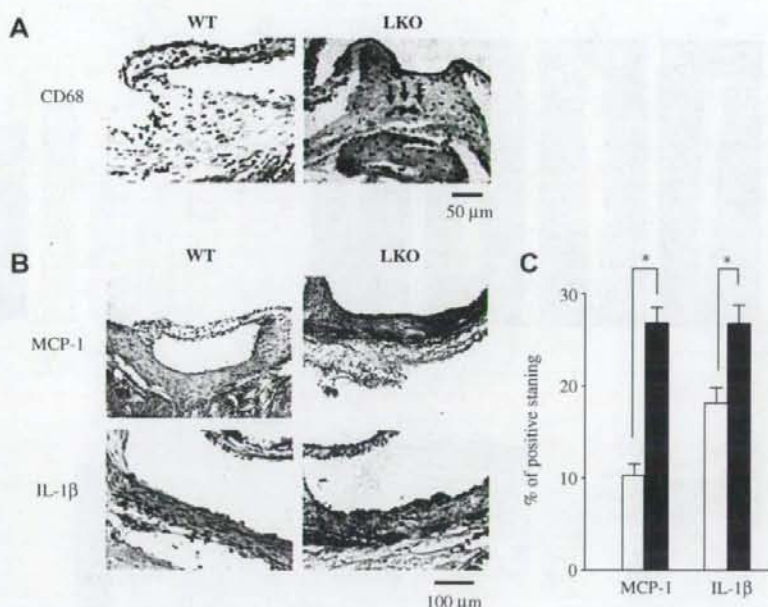
Fig. 3. (A) Immunohistochemical staining for CD68 in WT and LKO mice. Arrows indicate stained macrophages. (B) Immunohistochemical staining for MCP-1 and IL-1β in WT and LKO mice. (C) Quantitative analyses of the cell areas that stained positive for MCP-1 and IL-1β in WT mice (open bars) and LKO mice (closed bars). Data represent means ± SE for the percentage staining of the total plaque area in five sections for each animal ($n = 6$; $^*P < 0.01$).

progressed atherosclerosis. They attribute their results to differences in insulin resistance. Conversely, in our results, LKO mice fed a high-fat diet did not show differences in glucose homeostasis; however, they showed well-progressed atherosclerosis. Thus in our model, a mechanism other than insulin resistance seems to be associated with atherogenesis. One interesting possibility is the lack of a role of L-PGDS in inflammatory responses which play a central role in atherogenesis. The L-PGDS enzymatic product PGD_2 inhibits inducible nitric oxide synthase (NOS) [19] in vascular smooth muscle cells and suppresses the expression of pro-inflammatory mediators such as plasminogen activator inhibitor-1 [20] and vascular cell adhesion molecule-1 [21] in endothelial cells. 15d-PGJ_2 has also been shown to suppress inflammatory responses, which are dependent on or independent of PPARγ. 15d-PGJ_2 inhibits macrophage activation [22], production of monocyte inflammatory cytokines [23] and biologic functions of human natural killer cells [24]. 15d-PGJ_2 has also been shown to suppress inducible NOS expression [22]. In the present study, an increase in macrophage infiltration in the aortic root was observed in LKO mice. In support of this observation, the expression of MCP-1 which mediates monocyte recruitment to sites of inflammation and a pro-inflammatory cytokine, IL-1β, was enhanced in atherosclerotic lesions. These findings suggest that, in the vascular wall, l-pgds deficiency facilitates atherogenesis due to the lack of anti-inflammatory effects.

Taken together, we found that deletion of the l-pgds gene induces obesity in high cholesterol conditions in mice. l-pgds deficiency also resulted in highly progressed atherosclerosis by enhancing inflammatory responses. Our data suggest the potential anti-obese and atheroprotective effects of L-PGDS.

Acknowledgments

References

[1] Y. Kikawa, S. Narumiya, M. Fukushima, H. Wakatsuka, O. Hayaishi, 9-Deoxy-$\Delta^9,\Delta^{12-13,14}$-dihydroprostaglandin D_2, a metabolite of prostaglandin D_2 formed in human plasma, Proc. Natl. Acad. Sci. USA 81 (1984) 1317–1321.

[2] Y. Urade, O. Hayaishi, Prostaglandin D_2 and sleep regulation, Biochim. Biophys. Acta 1436 (1999) 606–615.

[3] O. Hayaishi, Y. Urade, Prostaglandin D_2 in sleep-wake regulation: recent progress and perspectives, Neuroscientist 8 (2002) 12–15.

[4] N. Eguchi, T. Minami, N. Shirafuji, Y. Kanaoka, T. Tanaka, A. Nagata, N. Yoshida, Y. Urade, S. Ito, O. Hayaishi, Lack of tactile pain (allodynia) in lipocalin-type prostaglandin D synthase-deficient mice, Proc. Natl. Acad. Sci. USA 96 (1999) 726–730.

[5] Y. Taba, T. Sasaguri, M. Miyagi, T. Abumiya, Y. Miwa, T. Ikeda, M. Mitsumata, Fluid shear stress induces lipocalin-type prostaglandin D synthase expression in vascular endothelial cells, Circ. Res. 86 (2000) 967–973.

[6] T. Sasaguri, Y. Miwa, Prostaglandin J_2 family and the cardiovascular system, Curr. Vasc. Pharmacol. 2 (2004) 103–114 (Review).

[7] B.M. Forman, P. Tontonoz, J. Chen, R.P. Brun, B.M. Spiegelman, R.M. Evans, 15-Deoxy-$\Delta^{12,14}$-prostaglandin J_2 is a ligand for the adipocyte determination factor PPAR gamma, Cell 83 (1995) 803–812.

[8] S.A. Kliewer, J.M. Lenhard, T.M. Willson, I. Patel, D.C. Morris, J.M. Lehmann, A prostaglandin J_2 metabolite binds peroxisome proliferator-activated receptor gamma and promotes adipocyte differentiation, Cell 83 (1995) 813–819.

[9] Y. Miwa, T. Sasaguri, H. Inoue, Y. Taba, A. Ishida, T. Abumiya, 15-Deoxy-$\Delta^{12,14}$-prostaglandin J_2 induces G_1 arrest and differentiation marker expression in vascular smooth muscle cells, Mol. Pharmacol. 58 (2000) 837–844.

[10] Y. Miwa, F. Takahashi-Yanaga, S. Morimoto, T. Sasaguri, Involvement of clusterin in 15-deoxy-$\Delta^{12,14}$-prostaglandin J_2-induced vascular smooth muscle cell differentiation, Biochem. Biophys. Res. Commun. 319 (2004) 163–168.

[11] N. Hirawa, Y. Uehara, M. Yamakado, Y. Toya, T. Gomi, T. Ikeda, Y. Eguchi, M. Takagi, H. Oda, K. Seiki, Y. Urade, S. Umemura, Lipocalin-type prostaglandin d synthase in essential hypertension, Hypertension 39 (2002) 449–454.

[12] K. Hamano, Y. Totsuka, M. Ajima, T. Gomi, T. Ikeda, N. Hirawa, Y. Eguchi, M. Yamakado, M. Takagi, H. Nakajima, H. Oda, K. Seiki, N. Eguchi, Y. Urade, Y. Uehara, Blood sugar control reverses the increase in urinary excretion of prostaglandin D synthase in diabetic patients, Nephron 92 (2002) 77–85.

[13] Y. Miwa, H. Oda, Y. Shiina, K. Shikata, M. Tsushima, S. Nakano, T. Maruyama, S. Kyotani, N. Eguchi, Y. Urade, F. Takahashi-Yanaga, S. Morimoto, T. Sasaguri, Association of serum lipocalin-type prostaglandin D synthase levels with

subclinical atherosclerosis in untreated asymptomatic subjects, Hypertens. Res. 31 (2008) 1939–1947.

[14] Y. Miwa, S. Takiuchi, K. Kamide, M. Yoshii, T. Horio, C. Tanaka, M. Banno, T. Miyata, T. Sasaguri, Y. Kawano, Identification of gene polymorphism in lipocalin-type prostaglandin D synthase and its association with carotid atherosclerosis in Japanese hypertensive patients, Biochem. Biophys. Res. Commun. 322 (2004) 428–433.

[15] T. Björnheden, B. Jakubowicz, M. Levin, B. Odén, S. Edén, L. Sjöström, M. Lönn, Computerized determination of adipocyte size, Obes. Res. 12 (2004) 95–105.

[16] E.M. Rubin, R.M. Krauss, E.A. Spangler, J.G. Verstuyft, S.M. Clift, Inhibition of early atherogenesis in transgenic mice by human apolipoprotein AI, Nature 353 (1991) 265–267.

[17] L. Ragolia, T. Palaia, C.E. Hall, J.K. Maesaka, N. Eguchi, Y. Urade, Accelerated glucose intolerance, nephropathy, and atherosclerosis in prostaglandin D_2 synthase knock-out mice, J. Biol. Chem. 280 (2005) 29946–29955.

[18] L. Ragolia, C.E. Hall, T. Palaia, Lipocalin-type prostaglandin D_2 synthase stimulates glucose transport via enhanced GLUT4 translocation. Prostaglandins Other Lipid Mediat. 87 (2008) 34–41.

[19] H. Nagoshi, Y. Uehara, F. Kanai, S. Maeda, T. Ogura, A. Goto, T. Toyo-Oka, H. Esumi, T. Shimizu, M. Omata, Prostaglandin D_2 inhibits inducible nitric oxide synthase expression in rat vascular smooth muscle cells, Circ. Res. 82 (1998) 204–209.

[20] H. Negoro, W.S. Shin, R. Hakamada-Taguchi, N. Eguchi, Y. Urade, A. Goto, T. Toyo-Oka, T. Fujita, M. Omata, Y. Uehara, Endogenous prostaglandin D_2 synthesis reduces an increase in plasminogen activator inhibitor-1 following interleukin stimulation in bovine endothelial cells, J. Hypertens. 20 (2002) 1347–1354.

[21] H. Negoro, W.S. Shin, R. Hakamada-Taguchi, N. Eguchi, Y. Urade, A. Goto, T. Toyo-Oka, T. Fujita, M. Omata, Y. Uehara, Endogenous prostaglandin D_2 synthesis decreases vascular cell adhesion molecule-1 expression in human umbilical vein endothelial cells, Life Sci. 78 (2005) 22–29.

[22] M. Ricote, A.C. Li, T.M. Willson, C.J. Kelly, C.K. Glass, The peroxisome proliferator-activated receptor-gamma is a negative regulator of macrophage activation, Nature 391 (1998) 79–82.

[23] C. Jiang, A.T. Ting, B. Seed, PPAR-gamma agonists inhibit production of monocyte inflammatory cytokines, Nature 391 (1998) 82–86.

[24] X. Zhang, M.C. Rodriguez-Galan, J.J. Subleski, J.R. Ortaldo, D.L. Hodge, J.M. Wang, O. Shimozato, D.A. Reynolds, H.A. Young, Peroxisome proliferator-activated receptor-gamma and its ligands attenuate biologic functions of human natural killer cells, Blood 104 (2004) 3276–3284.